Checkpoint kinase 2 (Chk2) inhibits the activity of the Cdc45/MCM2-7/GINS (CMG) replicative helicase complex

Ivar Ilves[1], Nele Tamberg[1], and Michael R. Botchan[2]

Division of Biochemistry and Molecular Biology, Department of Molecular and Cell Biology, University of California, Berkeley, CA 94720

This contribution is part of the special series of Inaugural Articles by members of the National Academy of Sciences elected in 2008.

Contributed by Michael R. Botchan, July 6, 2012 (sent for review May 24, 2012)

The replication of eukaryote chromosomes slows down when DNA is damaged and the proteins that work at the fork (the replisome) are known targets for the signaling pathways that mediate such responses critical for accurate genomic inheritance. However, the molecular mechanisms and details of how this response is mediated are poorly understood. In this report we show that the activity of replisome helicase, the Cdc45/MCM2-7/GINS (CMG) complex, can be inhibited by protein phosphorylation. Recombinant *Drosophila melanogaster* CMG can be stimulated by treatment with phosphatase whereas Chk2 but not Chk1 interferes with the helicase activity in vitro. The targets for Chk2 phosphorylation have been identified and reside in MCM subunits 3 and 4 and in the GINS protein Psf2. Interference requires a combination of modifications and we suggest that the formation of negative charges might create a surface on the helicase to allosterically affect its function. The treatment of developing fly embryos with ionizing radiation leads to hyperphosphorylation of Psf2 subunit in the active helicase complex. Taken together these data suggest that the direct modification of the CMG helicase by Chk2 is an important nexus for response to DNA damage.

eukaryotic DNA replication | S-phase checkpoint response

Propagation of genetic information through cell division is dependent on high-fidelity replication of each and every segment of genomic DNA before the resulting two copies of chromosomes are partitioned into daughter cells. This remarkable fidelity is achieved through multiple tiers, including highly accurate proofreading by DNA polymerases and many elaborate DNA repair pathways. Enormous progress has been achieved in unraveling the intricacies of these repair processes and the critical S-phase checkpoints that coordinate the DNA repair with the cell cycle. However, the details of how the replication machinery itself is affected during the S-phase checkpoint response remain a frontier area.

To ensure a timely completion of replication for the huge eukaryotic genome, a number of replication forks are initiated gradually throughout S phase from the potential start sites (origins) in genomic DNA (1). A critical step that is thought to be coordinate with the initiation of an active replisome is the activation of the replicative DNA helicase—the Cdc45/MCM2-7/GINS (CMG) complex (2–4). The core part of this complex—MCM2-7—is brought to chromosomes in late M or early G1 phases of the cell cycle as an inactive double hexamer that encircles the duplex DNA (5, 6). How the DNA duplex first melts and the MCM2-7 double hexamers separate to create two bidirectionally moving replication forks (7) is still unclear, but the proper interaction of GINS and Cdc45 with the MCM core to create an active CMG helicase is likely concomitant with this process (2, 8, 9). CMG helicase further unwinds the DNA strands in front of the replisome on the progressing fork, thus preparing the template for synthesis of nascent strands by DNA polymerase (10, 11).

The DNA replication-related S-phase checkpoint mechanisms have been most extensively studied in the simple eukaryote budding yeast (*Saccharomyces cerevisiae*), where the replication initiation step for later firing origins has emerged as a principal downstream target. The initiation of DNA replication in eukaryotes is controlled by two cell-cycle kinases: cyclin-dependent protein kinase (CDK) and Cdc7/Dbf4 protein kinase (DDK) (12). In response to DNA damage during S phase, the activated checkpoint kinase Rad53 shuts off DDK by phosphorylating its regulatory subunit Dbf4. Rad53 also phosphorylates and turns off Sld3, which is an essential downstream target of CDK signaling crucial for the assembly and activation of CMG helicase (13, 14). Hence, activation of the S-phase checkpoint in *S. cerevisiae* probably blocks the firing of late origins by blocking the formation of the CMG at these sites. The already assembled replisome complexes are targeted as well by S-phase checkpoints in budding yeast. Some of these mechanisms serve to ensure the integrity and stability of the replisome on the progressing fork, avoiding the disengagement of the helicase and polymerase complexes from each other and from the newly synthesized DNA strand when challenged by nucleotide shortage or damage in the template strand (15). Other replisome targeting checkpoint mechanisms may directly slow down the progressing fork. As an indication of this action, the direct Rad53- and Mec1 (upstream activator kinase of Rad53)-dependent inhibition of fork progression in response to hydroxyurea-induced S-phase checkpoint has been reported recently (16), albeit the molecular details behind this remain to be elucidated.

Vertebrate cells have also long been known to respond to DNA damage by blocking replication initiation as well as slowing the progressing replication forks (17–19). Proper execution of checkpoint responses is critical to avoid the development of neoplastic growth and mutations in checkpoint genes are often associated with cancer (20, 21). Metazoan Chk1 kinase and its main upstream activator kinase ATR (related to budding yeast Rad53 and Mec1, respectively) are essential checkpoint effectors in response to a wide variety of genotoxic insults. Two other metazoan checkpoint kinases—Chk2 and its main upstream activator ATM (homologous to Chk1/Rad53 and ATR/Mec1, respectively)—are primarily linked to the checkpoint response to double-strand DNA breaks (22, 23). Whereas Chk1 and Chk2 are thought to be active in somewhat distinct pathways, there is also evidence for an extensive crosstalk between ATM-Chk2 and ATR-Chk1 controlled checkpoint responses (24). The metazoan ATR-Chk1 pathway seems to control the replication initiation in a manner similar to that of the Mec1-Rad53 pathway in budding yeast, by negatively regulating the putative vertebrate homolog

Author contributions: I.I. and M.R.B. designed research; I.I. and N.T. performed research; N.T. contributed new reagents/analytic tools; I.I. and M.R.B. analyzed data; and I.I. and M.R.B. wrote the paper.

The authors declare no conflict of interest.

[1]Present address: Institute of Technology, Faculty of Science and Technology, University of Tartu, 50411 Tartu, Estonia.

[2]To whom correspondence should be addressed. E-mail: mbotchan@berkeley.edu.

This article contains supporting information online at www.pnas.org/lookup/suppl/doi:10.1073/pnas.1211525109/-/DCSupplemental.

of Sld3, Treslin/ticrr (25) as well as the DDK kinase in humans and *Xenopus* (26, 27). Very little is known about the replication elongation-related checkpoint mechanisms in metazoans.

We focused the present biochemical study on the regulation of the CMG by phosphorylation modifications. Cell-cycle kinases DDK and CDK are required upstream for activation of the CMG (12, 28–30) and several studies have described the checkpoint-dependent phosphorylation of CMG subunits (16, 31–35), but the effects or requirements for these modifications for activity or stability of CMG helicase remain largely unexplored. Results reported here demonstrate that the activity of the CMG complex is regulated by inhibitory phosphorylation and we have identified Chk2 kinase as a negative regulator of CMG helicase. Chk2 phosphorylates residues that are clustered to regions of low structural complexity in the MCM3, MCM4, and Psf2 subunits. Whereas the actual phosphorylated amino acids and neighboring sequences are themselves poorly conserved in primary sequence across phyla, the regions identified, particularly in Psf2 and MCM3, have maintained a composition and length proximal to well-conserved primary sequences and have been previously identified as regions for modification in damage response (34, 35). This demonstration that the activity of the eukaryotic replicative helicase holoenzyme can be directly regulated by a checkpoint kinase sets the stage for exploring a direct role for such mechanisms at the replisome, with a potential role in fork arrest or slowdown.

Results

Biochemical Activity of CMG Replicative Helicase Complex Is Regulated by Phosphorylation. We purified recombinant *Drosophila* CMG complex (2) and treated it with the nonspecific phosphatase from bacteriophage λ (λPPase). The treated CMG was separated from the λPPase by Mono-Q anion exchange chromatography that also resolves the full CMG from potentially incomplete combinations of its subunits that might arise from instability of the complex following phosphatase treatment. The vast majority of CMG survived the treatment with λPPase, as indicated by both the Mono-Q profile (Fig. S1*A*) and the gel filtration trace (Fig. S1*C*), where the complex runs as anticipated from previous analysis (2). We tested the helicase activity of λPPase-treated and repurified CMG side by side with mock-treated and repurified complex (Fig. S1*B*). As shown in Fig. 1*A* and quantified in Fig. 1*B*, the λPPase treatment resulted in a robust activation of the CMG helicase compared with the nontreated control. These data suggest that the reconstituted *Drosophila* CMG complex carries phosphorylation modifications that are inhibitory to its helicase activity.

Chk2 Checkpoint Kinase Phosphorylates CMG and Inhibits Its Helicase Activity. Baculovirus replication is known to induce DNA damage response in host cells (36, 37) and CMG subunits are phosphorylated in response to DNA damage in eukaryotes (16, 31–35). Therefore, we decided to focus our search on candidate checkpoint kinases that might regulate the CMG. We purified to near homogeneity two *Drosophila* enzymes, Chk1 and Chk2, using the baculovirus expression system. Both enzymes were able to autophosphorylate effectively in the presence of radioactive ATP as a phosphate group donor (Fig. 1*C*), indicative of active proteins. We found that Chk2, but not Chk1, phosphorylates the CMG in these assays. Moreover, the helicase activity of CMG was inhibited by the presence of Chk2 kinase in a concentration-dependent fashion. Both the more active λPPase-treated and untreated CMG complexes were inhibited equally by Chk2 (Fig. 1*D* and quantification in Fig. 1*E*).

We detected three bands specific to the CMG after Chk2 modification and autoradiography of the SDS/PAGE gel (Fig. 1 *C* and *F*, *Left*, bands I–III). Prior treatment of the CMG with λPPase did not affect the specific bands modified (Fig.1*F*, *Left*, compare "no PPase" to "PPase" in autoradiographs). The quantification of radioactive phosphate incorporation showed the same levels of phosphorylation as a function of Chk2 concentration in phosphatase-treated compared with untreated CMG for each subunit target (Fig. S1*D*).

Chk2 Phosphorylates MCM3, MCM4, and Psf2 Subunits and the Target Sites Are Clustered to Short Patches. The alignments of the autoradiographs with the silver-stained protein gels indicate that Chk2 target subunits II and III are likely Psf2 and MCM4. We created recombinant expression vectors to produce deletions of these subunits in regions suspected to contain the modification domains. The truncations removed the final 33 C-terminal amino acids of Psf2 and the first 141 N-terminal residues of MCM4; both of these regions contain multiple serine and threonine residues in all species but show relatively poor conservation when aligned to otherwise very homologous MCM proteins from other eukaryotes (Fig. S2). Such protein regions are frequently involved in modifications when addition of charge by phosphorylation rather than a very specific structure is an essential component of regulation (38). The corresponding C-terminal tail of human Psf2 protein did not resolve into a defined atomic structure in all three published crystal structures of the GINS (39–41). The N-terminal tail of MCM4 deleted in the subsequent experiments is also a known phosphorylation target and falls outside of the conserved region in eukaryotic MCM proteins where the structures can be threaded readily onto the available crystal structures of homologous archeal MCM protein (42, 43). The truncated MCM4 and Psf2 subunits were incorporated into the full CMG complex both alone (Fig. 2*A*, lanes MCM4ΔN and Psf2ΔC) and in combination (Fig. 2*A*, lane MCM4ΔN Psf2ΔC). We tested the Chk2 phosphorylation patterns of the purified mutant CMG complexes. The radioactively labeled protein bands were visible on the lanes where WT Chk2 was used (Fig. 2 *A* and *B*, *Left*, lanes marked "+"), but not on the lane with kinase-defective point mutant Chk2 (Fig. 2*A*, lane marked "mut"). The truncated Psf2 and MCM4 subunits displayed faster mobility on SDS/PAGE (Fig. 2*A*, bands Psf2ΔC and 4ΔN in silver-stained gels) and the truncation of either subunit alone or in combination led to the disappearance of respective bands from the autoradiograph (Fig. 2*A*). This result supported our assignments for two of the Chk2 target subunits as Psf2 and MCM4 and possibly mapped the phosphorylation target regions to the truncated tails (Fig. 2*E*).

The third phosphorylation band in the autoradiograms (Fig. 1*F*, band I) had the same mobility as comigrating MCM3 and MCM6 proteins. To clarify the potential target(s), we tagged either an MCM3 or an MCM6 subunit with a bulky maltose-binding protein (MBP) moiety and purified the respective CMG complexes (Fig. 2*B*, compare bands 3;6 to 3;6+MBP in the silver-stained total protein gel). These experiments identified MCM3 as the sole site for modification (Fig. 2*B*, compare lanes MCM3+MBP and MCM6+MBP).

Quantification of the radioactive phosphate incorporation revealed that all three target subunits were modified to the same extent: 0.7–0.9 phosphates were added on average per subunit in saturating conditions (Fig. 2*C*, quantified in Fig. 2*D*). Also, the Psf2 protein band became fully shifted at the saturating kinase concentrations, indicating that at least one phosphate has been added to every Psf2 protein molecule (Fig. 2*C*, *Right*; nonphosphorylated Psf2 band is indicated by an arrow; note that the shifted phospho-Psf2 band is masked by one of the creatine kinase bands indicated by asterisks). The phospho-Psf2 bands have different mobility shifts dependent on the Chk2 concentration in the reaction mix (Fig. 2*C*, *Left*; compare lanes with 10, 50, and 150 nM Chk2 in the autoradiograph). This result means that the quantified results may be an underestimation (e.g., due to the free radioactive phosphate contamination in the used [γ-^{32}P]ATP) or these different bands may correspond to Psf2 proteins carrying different single-residue modifications that confer different electrophoretic mobility to Psf2 protein and are modified by Chk2 in a concentration-dependent fashion ("low-affinity" and "high-affinity" sites).

To map directly the target region(s) for phosphorylation in MCM3 and to precisely define our assignments from the other CMG members, we performed a mass spectrometry analysis of

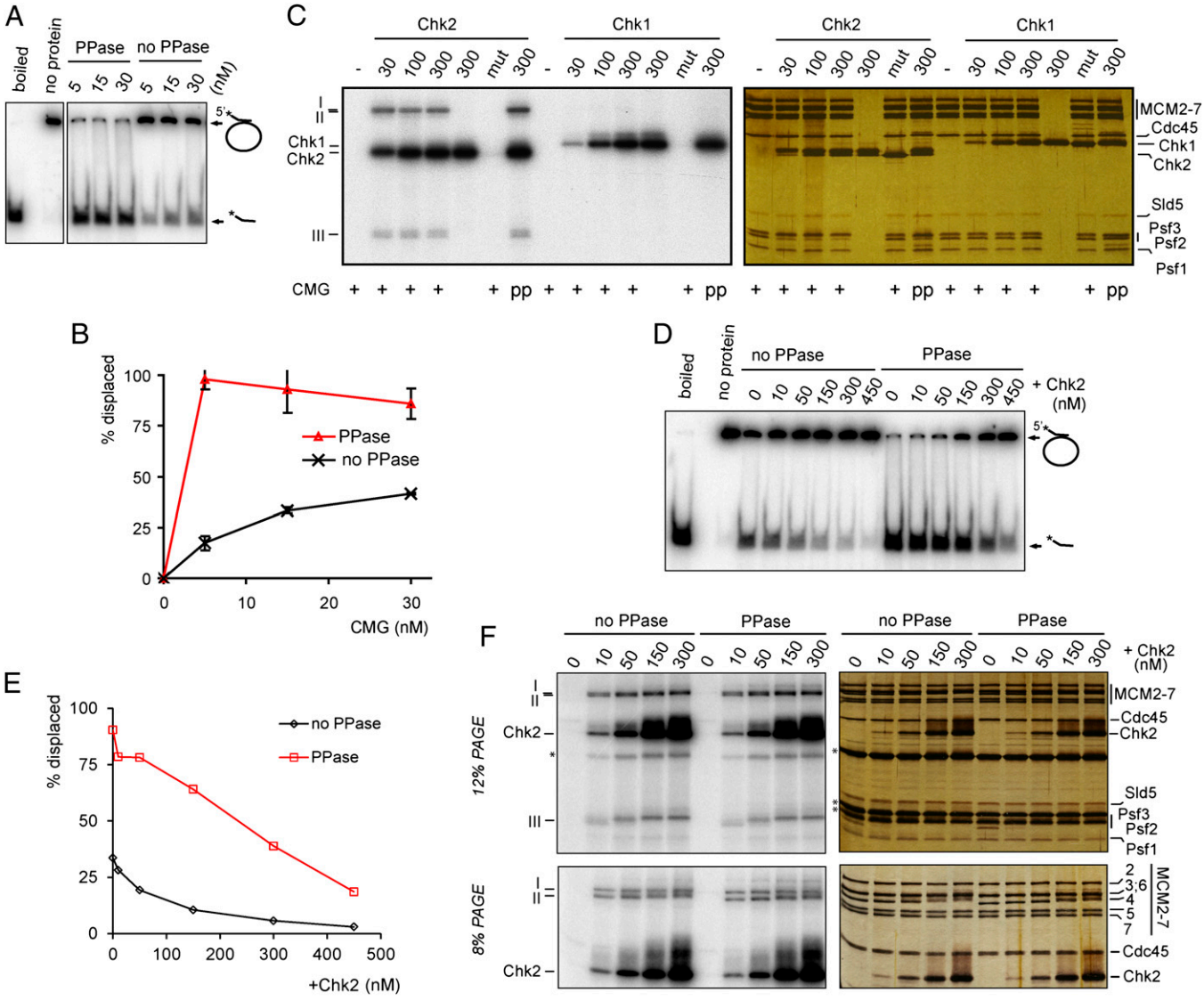

Fig. 1. Phosphatase treatment activates and Chk2 phosphorylation inhibits the CMG helicase. (*A*) Autoradiograph of the helicase assay products resolved on PAGE. λ-Phosphatase–treated and repurified CMG (PPase) was compared with mock-treated complex (no PPase). The positions of starting double-stranded substrate and displaced oligonucleotide bands are indicated by arrows. The concentration of CMG is given on top of each lane. "Boiled" and "no protein" indicate control lanes with heat-denatured substrate and substrate without protein, respectively. (*B*) Quantified data of two independent helicase assays. Percentage of displaced oligonucleotide is plotted as a function of CMG concentration. Error bars show SD. (*C*) Kinase assay showing the phosphorylation of purified CMG (30 nM) with various concentrations of Chk1 or Chk2 as indicated on top (nM). The reaction products were resolved in 12% SDS/PAGE before silver staining and exposing to film. Here and in *F*, the silver-stained gel is shown at *Right* and the autoradiography of the same gel at *Left*. "mut" indicates lanes corresponding to control reactions with kinase-defective mutant proteins, both 300 nM. "+" at the bottom of the lane indicates the presence of CMG in the reaction; "pp" marks reactions with λ-phosphatase–treated CMG. The bands of CMG that become radiolabeled due to the phosphorylation by Chk2 (I–III), and the Chk1 and Chk2 autophosphorylation bands are marked on the left. (*D*) Helicase assay with phosphatase-treated CMG (20 nM) that was pretreated for 10 min with indicated concentrations of Chk2 before DNA substrate was added. (*E*) Quantified data from *C*, showing the percentage of oligonucleotide displaced as a function of Chk2 concentration in reaction. (*F*) Kinase assay with 20 nM CMG incubated with indicated concentrations of Chk2 in the presence of radiolabeled ATP. Incubation time (30 min) was chosen to ensure the near saturation of radioactive phosphate transfer. Half of each reaction was run on 12% PAGE (*Upper*) and another half on 8% PAGE (*Lower*). The bands of CMG that become radiolabeled due to the phosphorylation by Chk2 (I–III) and the Chk2 autophosphorylation band (Chk2) are marked on the left. Asterisks mark the bands corresponding to a creatine kinase that was added as a part of the ATP regeneration system in this assay.

the Chk2-phosphorylated CMG. The Chk2-treated CMG was prepared using heavy isotopic [^{18}O]ATP as a phosphate donor, which allows us to distinguish the phosphates added by Chk2 kinase from the phospho-groups that were already present in the purified complex. For MCM3, we found that 10 residues were potential phosphorylation sites for Chk2, 8 of these residues clustering to a region in the C-terminal domain of the protein that is situated between the well-conserved AAA$^+$ and C-terminal end domains (Fig. S2 and Fig. 2*E*). Mass spectrometry analysis mapped, as anticipated from the data presented above, multiple Chk2 phosphorylation sites also to the N-terminal region of MCM4 and the C-terminal end of Psf2 (Fig. S2). Interestingly, in each of the scored phosphopeptides, only one of the residues was found to be modified by the kinase. This, together with the fact that the estimated number of residues modified per subunit at saturation appeared to be lower than the total number of all identified candidate sites in a subunit, suggests that only a small number of residues (at least one) from

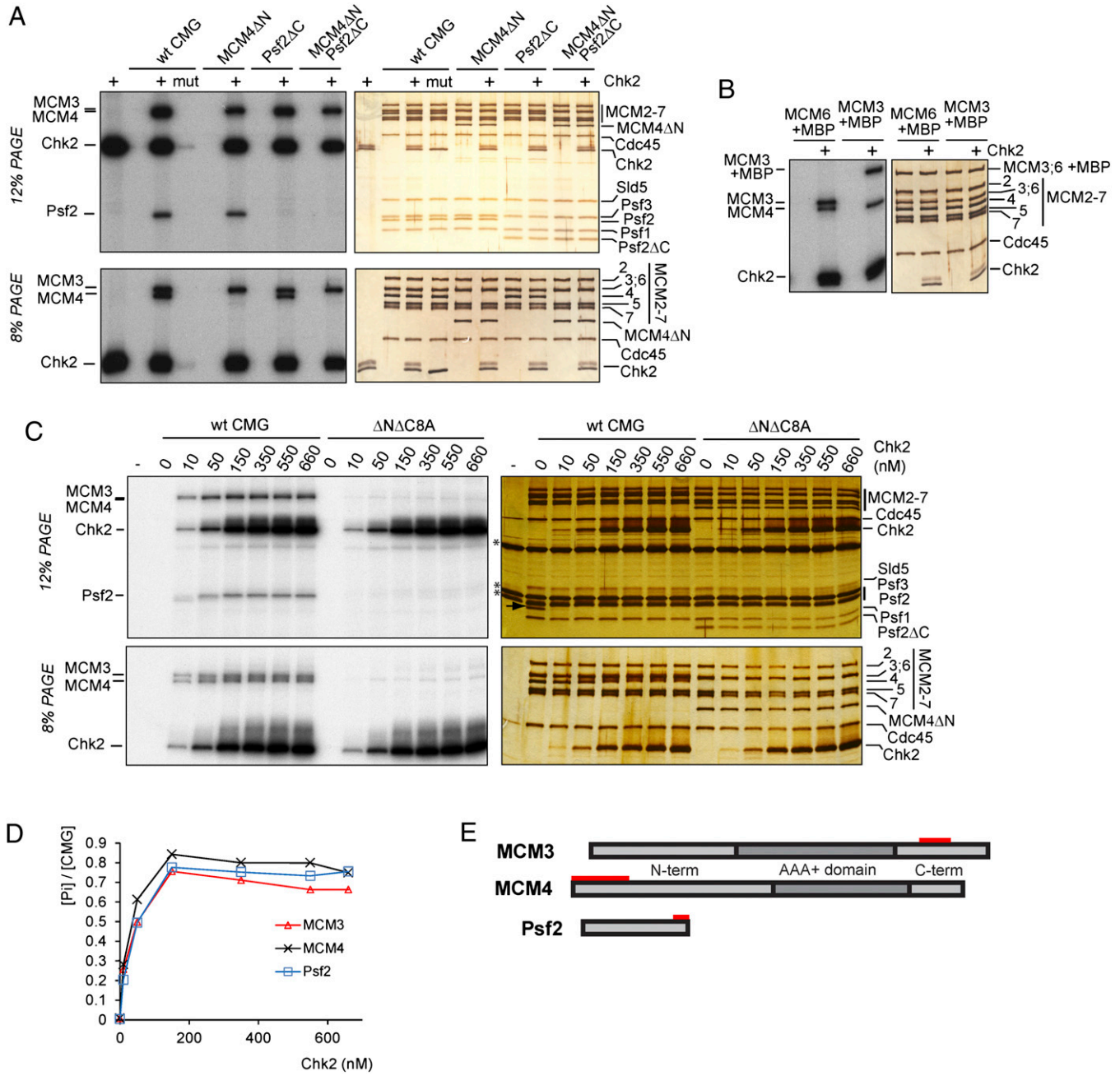

Fig. 2. Chk2 phosphorylates specific regions in MCM4, MCM3, and Psf2 subunits of CMG. (*A*) Kinase assay with Chk2 and CMG complexes containing truncated Psf2 or MCM4 subunits. Half of each reaction was run on 12% PAGE (*Upper*) and another half on 8% PAGE (*Lower*). The addition of Chk2 is indicated by "+" and "mut" marks the lanes corresponding to reactions with kinase-defective Chk2. A total of 100 nM Chk2 was used to phosphorylate 30 nM CMG in these reactions. (*B*) Chk2 phosphorylation of CMG complexes containing MBP-tagged MCM3 or MCM6 subunits. Eight percent PAGE was used to resolve the MCM region. (*C*) Kinase assay with WT CMG compared with triple-mutant CMG. Chk2 concentrations are as indicated on top; "-" marks a control lane with reaction buffer and no CMG or Chk2. Asterisks mark the creatine kinase bands; arrow on the silver-stained gel indicates the mobility of non-phosphorylated Psf2 protein. Reactions were resolved in a 12% PAGE/SDS gel. (*D*) The average number of radioactive phosphates transferred per each of the target subunits plotted as a function of Chk2 concentration in the reactions. The estimate of phosphate incorporation was based on parallel calibration of the PhosphoImager quantification with the predetermined amounts of radioactive ATP. The data were quantified from the autoradiographs shown in *C*. (*E*) Schematic of the three identified Chk2 target regions (marked in red) in CMG subunits.

a list of potential target sites are selected by Chk2 for phosphorylation. The analysis for MCM3, which was the most extensive, did not show any one of the sites as preferred. We speculate that target choice within this domain is random and constrained by the location of a docking site for the kinase in the CMG. Interestingly, the alignment of respective proteins from closely related species of the Drosophilidae family shows that the Chk2 target regions in Psf2 and MCM3 form what is the least homologous region embedded in otherwise essentially identical proteins (Fig. S3).

We created an MCM3 expression vector with point mutations converting all eight of the clustered Chk2 target residues to alanine. In combination with the truncations of the tails in MCM4 and Psf2, it resulted in a CMG complex that was resistant to the

phosphorylation by Chk2 (Fig. 2*C*, *Left*, compare lanes wt CMG to lanes ΔNΔC8A in the autoradiograph).

Chk2 Inhibits CMG Helicase Through Phosphorylation-Dependent and -Independent Mechanisms. Plotting of the relative helicase activity of CMG against the concentration of WT Chk2 in the reaction indicated a striking Chk2-dependent inhibition of CMG activity (Fig. 3*A*, wt Chk2). For the mutant Chk2, which has its catalytic aspartic acid residue replaced by asparagine, the protein was unable to modify CMG subunits (Fig. S4*A*), but was able to inhibit the helicase activity of CMG at high concentrations (Fig.3*A*, mut Chk2). The shape of the interference plot for the mutant Chk2 was almost linear with kinase concentration and clearly less effective at lower concentrations. This result suggested that the inhibition of the CMG helicase activity by WT Chk2 results from both phosphorylation-dependent and -independent activities. To confirm this point, when we tested the phosphorylation-resistant mutant CMG complex in a similar set of experiments, we observed the same linear concentration-dependent inhibition of helicase activity by both the WT and the kinase-defective Chk2 (Fig. S4 *B* and *C*, compare wt Chk2 to mut Chk2).

To establish that the Chk2 modifications alone are sufficient to inhibit the CMG helicase, we phosphorylated the CMG with Chk2 and repurified the modified complex away from the kinase, using ion exchange chromatography. The mobility shift of phosphorylated Psf2 in an SDS/PAGE gel indicated efficient phosphorylation of kinase-treated complex (Fig. 3*B*, Psf2-Pi points to the slower-moving phosphorylated Psf2 band) and the chromatography results did not indicate any destabilization of the complex after the Chk2 phosphorylation. We also purified the control CMG that was treated with the kinase-defective Chk2 mutant. Fig. 3*C* shows that the helicase activity of the Chk2-phosphorylated CMG is indeed inhibited even without the continued presence of the kinase (compare CMG-Pi, the WT Chk2-modified and repurified complex, to CMG, the Chk2 mutant-treated control).

As the phosphorylation-independent component of the Chk2 inhibition of CMG was proportional to the concentration of kinase in the reaction mix, we surmised that this relationship was due to the direct interaction of the kinase with CMG. Immunoprecipitation assay with purified proteins revealed that the CMG indeed associates with Chk2. This interaction is not affected by the truncations and substitutions that remove the Chk2 phosphorylation sites from the CMG complex as the triple-mutant version associates with Chk2 as efficiently as WT CMG (Fig. 3*D*).

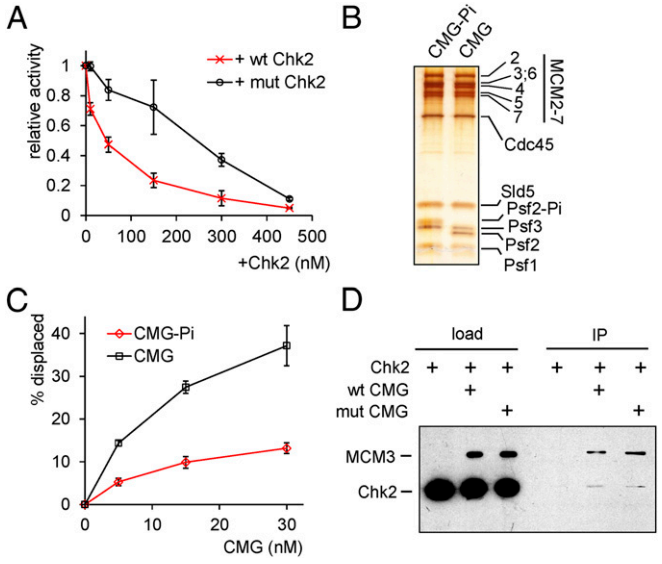

Fig. 3. Chk2 inhibits CMG helicase through both phosphorylation-dependent and -independent mechanisms. (*A*) Quantified data from two independent assays showing the helicase activity relative to the control reaction without Chk2. A total of 20 nM CMG was incubated in the presence of shown concentrations of WT Chk2 or kinase-defective mutant Chk2. (*B*) Silver-stained 12% SDS/PAGE gel shows the Chk2-phosphorylated and repurified CMG (CMG-Pi) side by side with untreated control (CMG). (*C*) Quantified data from two independent helicase assays comparing the Chk2-phosphorylated CMG to the untreated control CMG. (*D*) Western blot of the coimmunoprecipitation assay with purified Chk2 and either WT or phosphorylation-defective triple-mutant CMG. "Load" indicates the lanes with 1/20th of starting mix, and "IP" shows lanes with half of each coimmunoprecipitated product. Anti-Cdc45 antibodies were used to pull down the complexes; anti-flag monoclonal antibody was used to recognize the flag-tagged Chk2 and MCM3 proteins.

Phosphorylation of all Three Chk2 Target Subunits in CMG Contributes to the Inhibition of Helicase Activity. To examine the contribution of each of the Chk2 target subunits in CMG to the overall inhibitory effect on the helicase activity, we purified CMG complexes with all single and double combinations and the triple combination of phosphorylation mutant subunits (Fig. 4*A*). Relative inhibition of the helicase activity by Chk2 was then determined by measuring the helicase activity of purified complexes either with or without coincubation with Chk2 kinase. A single-kinase concentration was used in these experiments, where both the kinase binding and phosphorylation contribute to the inhibition. A CMG complex with one phosphorylation domain removed was less inhibited by Chk2 pretreatment than was WT CMG (Fig. 4*B* shows the fraction of helicase activity retained: 1.0 corresponds to no effect and 0 to complete inhibition). The Chk2-dependent inhibition of all three double-mutant complexes was even less efficient, close to that of the triple-mutant CMG. We conclude from this that the phosphorylation of each one of the three target subunits contributes similarly to the inhibition of the CMG helicase. In addition, the phosphorylation of at least two Chk2 target subunits of three is required for the most efficient phosphorylation-dependent inhibition of activity.

We also examined the helicase activity of CMG containing the phosphomimetic aspartic acid substitutions in the clustered eight Chk2 target sites in MCM3. The CMG with MCM3 8D subunit showed lower helicase activity than WT complex (Fig. 4*C*), but the difference was significantly smaller than that detected with the Chk2-phosphorylated and repurified CMG carrying modifications of all three target subunits (Fig. 3*C*). This result is consistent with the observations made in the case of phosphorylation-defective CMG complexes above.

Psf2 Subunit in the CMG Is Phosphorylated in *Drosophila* Embryos in Response to Ionizing Radiation. An immediate question was whether checkpoint activation induces the modification of the same CMG subunits as Chk2. We focused our attention on Psf2, as the phosphorylation of this subunit leads to shifted mobility in SDS/PAGE that can easily be detected by Western blotting (e.g., Fig. 3*B*).

We collected *Drosophila* embryos that were homozygous for an extra copy of flag-tagged MCM3 and treated one batch of these to 40 Gy of ionizing radiation (IR), comparing it to an equal untreated control. This level of radiation was shown to be sufficient to induce the cellular DNA damage response and Chk2 phosphorylation of known targets, the latter being indicative of the checkpoint-dependent activation of the kinase (44). Flag-tagged MCM3 containing MCM and CMG complexes was isolated from these embryo nuclear extracts by anti-flag immunoaffinity pull-down followed by size fractionation by Superose 6 gel filtration. As shown in Fig. 5*A*, the coelution of flagMCM3 with MCM2 and MCM4 subunits peaks in fractions 13–14, which corresponds to the hexameric MCM2–7 complex with the estimated molecular mass of 545 kDa (compare with the elution of molecular mass standards). The peak of flag-MCM3 in fractions 15–17 likely corresponds to the monomeric protein and MCM3-MCM5 heterodimers. The CMG complex in contrast peaks around fraction 12, as established by a Western blot analysis with

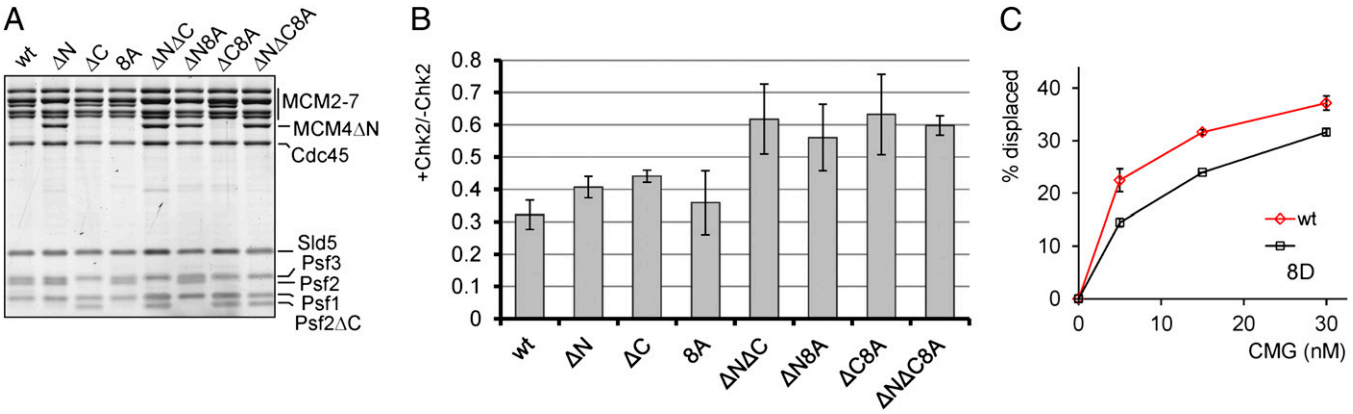

Fig. 4. Contributions of individual Chk2 target regions in CMG to the Chk2-dependent inhibition of CMG helicase. (*A*) SYPRO orange-stained 10% SDS/PAGE gel shows the purified CMG complexes. ΔN, ΔC, and 8A correspond to the complexes with truncated MCM4, Psf2, and point-mutated MCM3 subunits, respectively. (*B*) Quantified data from helicase assays show the effect of Chk2 addition on the activity of WT and mutant CMG complexes. Each column shows the fraction of helicase activity that is retained after pretreatment of respective CMG complexes with Chk2. The data were collected from three independent series of experiments. Two different protein preparations of WT, 8A, and ΔNΔC8A CMG complexes were tested in two of these series, with no apparent preparation-to-preparation variation. The concentrations of CMG and Chk2 proteins in the reactions were 20 nM and 150 nM, respectively. (*C*) Quantified data from two independent helicase assays comparing the activity of WT CMG (wt) to the CMG that carries phosphomimetic substitutions of Chk2 target residues in its MCM3 subunit (8D). The average percentage of processed substrate is presented as a function of CMG concentration in the reaction mix.

antibodies against Cdc45 and Psf2 subunits. These proteins are in complex with MCM3 when part of the full CMG complex and peak with the anticipated mobility of the CMG (711 kDa). Notably Psf2 in the CMG from irradiated fly embryos showed a double band in SDS/PAGE, whereas almost all Psf2 from the nontreated control was contained in a single band (Fig. 5*A*). Treatment of CMG peak material from fraction 12 with either λ-phosphatase or calf intestine alkaline phosphatase resulted in the loss of the upper slower-migrating band (Fig. 5*B*). This result indicates that the slower mobility results from the phosphorylation of Psf2. We conclude that Psf2, one of the Chk2 target subunits in CMG in vitro, is also phosphorylated in response to ionizing radiation-induced DNA damage and checkpoint response in the *Drosophila* embryos in vivo, while part of the full CMG holoenzyme complex.

Discussion

We have used purified proteins and an in vitro approach to show that phosphorylation directly regulates the activity of the replicative CMG helicase. Phosphatase treatment of the recombinant CMG leads to a marked enhancement, whereas Chk2 modifications inhibit the activity. These results suggest that modifications of the accessible surfaces and tails of the CMG helicase proteins are regulatory rather than critical for functioning of the complex, although they might be important for the assembly of the active replication fork. Our results lead to the suggestion that the DNA replication checkpoint pathways can directly regulate the enzymatic activities on the replication fork and reveal a potential role for Chk2 protein kinase in this process. *Drosophila* Chk2 kinase is an upstream activator of the Dmp53 important in cellular response to IR (44). In *Drosophila* as in other metazoans, the apoptotic response works through a signaling pathway that controls the transcription of genes important for this process. The *Drosophila* Chk1 homolog does not play a role in this pathway as it does in vertebrates (45). It is intriguing that IR can induce an apoptotic response in the absence of either Chk2 or p53 in *Drosophila*, but this response is very slow compared with the canonical pathway (46). Perhaps the absence of the S-phase response that slows down or halts the fork until repair can be mediated may lead to a distinct genetic imbalance that is eventually toxic to cells. Buttressing this idea is the finding that in imaginal discs, where IR induces apoptosis, DNA repair genes including

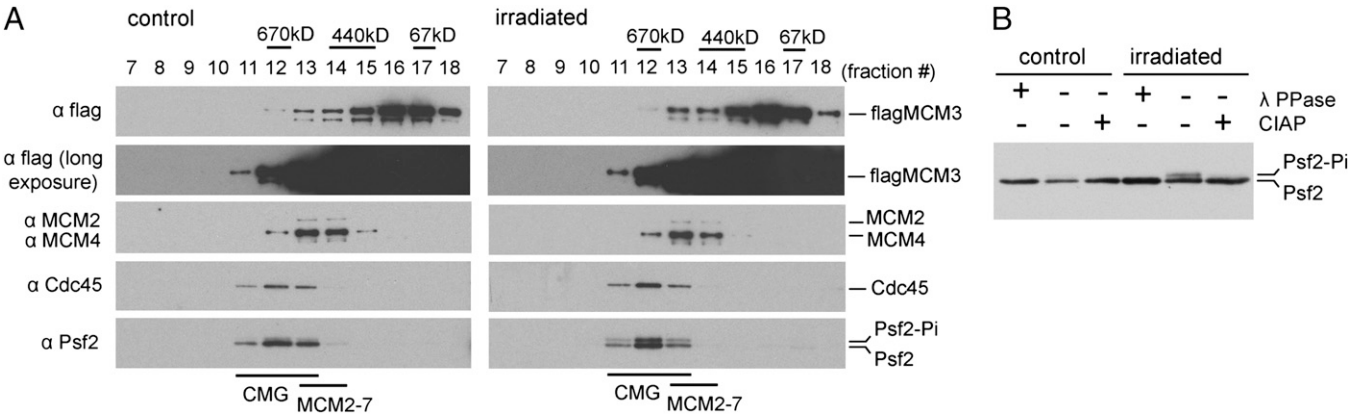

Fig. 5. Psf2 subunit of CMG is phosphorylated in *Drosophila* embryos in response to IR treatment. (*A*) Western blot of the flagMCM3 protein complexes separated on Superose 6 size exclusion chromatography. Fraction numbers and the elution of molecular weight standards are indicated on top of respective lanes. The CMG and MCM2-7 peak fractions are marked. (*B*) The Psf2 Western blot of the material from the CMG peak fraction no. 12 of the irradiated or control embryos treated with either λ-phosphatase (λ PPase) or calf intestine alkaline phosphatase (CIAP).

those specific to nonhomologous end joining are induced in a Chk2-dependent manner (44). Perhaps in those cells where the DNA damage is not at the threshold to induce apoptosis, the Chk2 modifications on the fork work in parallel for survival with p53-activated pathways.

We have shown that Psf2, one of the Chk2 targets in vitro, is phosphorylated in response to IR in embryos and that this modification is present in the assembled CMG complex. Given that the stable and biochemically tractable levels of the CMG are found only on active forks (4, 10, 11), we speculate that these modifications are relevant to the S-phase checkpoint regulation of replisome progression. Such a regulation might be amplified in the context of a full replisome where other proteins that are attached to the helicase may also be modified. This action might occur *in cis* to a double-strand break in DNA or even *in trans* to slow down all forks, even those far from a lesion. A global slowdown or stopping of the replication may be important for preventing the progressing replication forks from reaching the damaged sites in template DNA, thus avoiding a possible fork collapse.

All three Chk2 target regions identified in the CMG—long N-terminal tail of MCM4, C-terminal tail of Psf2, and a short stretch in the carboxyl-terminal domain of MCM3—have been previously reported as modified by checkpoint-related kinases. Two ATM and ATR consensus sites (SQ/TQ) are phosphorylated in the corresponding region of human and mouse Psf2 in response to ionizing or UV radiation (34). For the MCM proteins, ATM/ATR candidate phosphorylation sites are modified in response to treatment with DNA-damaging agents in the same region of human and mouse MCM3 protein (34, 35) (Fig. S2) and MCM4 has been found to be phosphorylated in response to checkpoint activation likely through the ATR-Chk1–dependent pathway (33). The residues modified cluster to the regions with limited sequence homology and characterized by low structural complexity. This modification suggests a robust or overlapping set of negative regulatory networks, which converge to a specific region of the holoenzyme for a common mechanism for inhibition. Electron microscopy reconstructions of the *Drosophila* CMG show that the target domains within both Mcm3 and Psf2 lie in proximity on the same face of the complex (9). The Mcm4 amino-terminal domain is predicted to be unstructured and, when fused to MBP tag, can lie to an extended trajectory away from the complex (9). However, without a tag and in the context of a bound DNA fork, the CMG may tie this very long tail to a region close to the interface provided by the other Chk2 targets. Hence a threshold may be imposed wherein at least two of the targets and perhaps all three may require modifications to create an allosteric change affecting a function, a common theme in protein regulation where unstructured domains can impose a regulatory change through modification (38, 47). The long and possibly flexible amino terminus of MCM4 may play multiple roles in the S-phase regulation given its importance as a critical phosphorylation target for the DDK kinase in budding yeast (29). The domain of MCM4 in this context may be perhaps tethered in a different structure specific to the MCM2–7 double hexamers.

Modifications of the replicative helicase may have additional roles in affecting the stability and composition of the replisome or remodel interactions with other enzymes. One intriguing prospect could be the role for checkpoint-dependent phosphomodifications in the coordination of stalled replication forks for a restart through pathways akin to break-induced replication (BIR). In budding yeast, BIR requires all components of the CMG (48). In one scenario phosphorylation status might allow for local reassembly at a break without recruitment from a free pool of proteins. A recent study in the *Xenopus* system has demonstrated that the CMG helicase reassembles during such fork rescue and involves partial disassembly of the complex as an intermediate step (49). Phosphorylation may assist in this process to first prevent nonproductive progression on the template. We found that the phosphorylation per se does not destabilize the CMG, so other regulatory proteins might be recruited to the forks and assist temporary disassembly for later reassembly and reloading. Proper modification of the fork components may be obligatory for such a step, as we have found that the CMG can bind to forked DNA in vitro without any assistance (2). In other situations, the full disassembly of the CMG complex might not always be required for its reloading after the fork rescue.

The utility of the biochemical approach is illustrated by the fact that the potential role of Chk2 in the direct regulation of the replisome had not been readily predicted from previous studies on the replication checkpoint in higher eukaryotes. It is rather the homologous Chk1 kinase that has emerged as a critical mediator of S-phase checkpoint response to DNA damage and the Chk1 gene is essential for viability in metazoans. The Chk2 gene, on the other hand, is nonessential in studied metazoans (24). This result has suggested a redundancy between Chk2 and the closely related Chk1. Despite this overlap in function, the Chk2 gene is broadly conserved, indicating that it executes roles that are crucial for the organism. To what extent this selection works solely in the checkpoint response to double-strand breaks is difficult to address. The importance of the Chk2 kinase in cellular homeostasis is emphasized by the established link to its role as a tumor suppressor where certain and a very specific class of mutations lead to predisposition for various cancers (50). Chk2 null mice do not develop spontaneous tumors without additional genotoxic treatment, but the mice expressing the kinase-deficient version of Chk2 in mammary glands do develop mammary tumors spontaneously (51). The knock-in mouse with the human cancer predisposing Chk2*1100delC allele develops tumors with high frequency even without additionally induced genotoxic stress (52). If we posit that Chk2 binds to important targets (e.g., in the replisome) that overlap with targets for Chk1 or other checkpoint kinases and that a defective Chk2 allele can thus provide a dominant-negative interference with critical steps in damage response that would not happen in a null allele, an interesting model presents that can be tested. In any case we suspect that specificity is provided by individual kinases to ensure the finely tuned pattern of modifications essential to customize responses to a range of different stress conditions.

Materials and Methods

Protein Purification and Coimmunoprecipitation Assay. All of the proteins were expressed using the Invitrogen Bac-to-Bac baculovirus system and purified from baculovirus-infected insect cells as described previously (2). The modifications in the purification protocol for Chk1 and Chk2 proteins and the methods for preparation of phosphatase or Chk2-treated and repurified CMG complexes are described in *SI Materials and Methods*.

In protein coimmunoprecipitation assays, 20 pmol of Chk2 was incubated with 1 pmol of CMG in buffer A (2) in the presence of 250 μg/mL insulin as a crowding agent (50 μL) with gentle mixing at room temperature for 30 min. Five microliters of packed protein A Sepharose CL-4B beads with cross-linked anti-Cdc45 peptide B antibody (4) was added in a total volume of 100 μL and incubated with end-over-end mixing for 2 h at 4 °C. The beads were washed four times with buffer C + 150 mM KCl. Bound proteins were eluted with 20 μL pH 2.5 glycine buffer (50 mM glycine, 150 mM NaCl) and immediately neutralized with 2 μL of 1 M Tris HCl, pH 8.0 before standard Western blotting analysis.

In Vitro DNA Helicase and Protein Phosphorylation Assays. The DNA helicase activity was measured as ability to displace the radiolabeled oligonucleotide from M13 genomic DNA as described in ref. 2, with the following differences. A total of 300 μM ATP in the reaction mix was supplemented with an ATP regeneration system (10 mM sodium creatine and 1 unit creatine phosphokinase; Sigma-Aldrich) and in the Chk2 addition experiments, the DNA substrate was added after preincubating the reactions for 10 min at 30 °C (20 min in the experiment in Fig. 4*B*). All of the helicase reactions were carried out for 30 min at 30 °C and stopped by adding standard SDS/EDTA loading dye and then treated for 20 min with 0.5 unit of proteinase K at 37 °C before loading on a polyacrylamide gel for resolving the reaction products.

The protein phosphorylation was carried out in the same reaction buffer as in the helicase assays, except that the DNA substrate was omitted and 300 μM ATP was spiked with [γ-^{32}P]ATP (10 μCi per reaction). A total of 100 μM ATP without the ATP regeneration system was added in the assays in Figs. 1*C* and 2 *A* and *B*. The reactions were incubated 30 min at 30 °C (except 20 min in Fig. 1*C*), before the proteins were resolved on SDS/polyacrylamide gel

electrophoresis. The gel was silver stained, dried on Whatman paper, and exposed to an autoradiography film. To estimate the phosphorylation efficiency, known amounts of radioactive ATP in the starting reaction mix were spotted on the filter paper and coexposed to the PhosphoImager cassette (GE Healthcare) as a calibration standard. To map the sites in CMG complex phosphorylated by Chk2, the reactions were carried out in the presence of 1 mM [^{18}O]ATP and both the insulin and the ATP regeneration system were omitted from the mix. Following trypsin digestion of the samples, mass spectrometry analysis of the phosphosites was carried out by Lori Kohlstaedt in the Vincent J. Coates Proteomics/Mass Spectrometry Laboratory at University of California, Berkeley.

Fractionation of *Drosophila* Embryo Extracts. The transgenic *Drosophila* strain homozygous for the P element that expresses flag-tagged MCM3 cDNA was created by Stephen Moyer (University of California, Berkeley, CA). The collection trays with 0- to 12-h *Drosophila* embryos were harvested from the population cages over the span of 3–4 d and stored at 4 °C until the last collection, when the embryos were harvested and pooled at the room temperature. One-half of the embryos were then exposed to 40 Gy of ionizing radiation, the other half serving as an untreated control, and the nuclear extracts were prepared as described previously (4). The CMG-containing high molecular mass fractions were isolated using the combination of immunoaffinity purification and gel filtration steps as described in *SI Materials and Methods*.

ACKNOWLEDGMENTS. We thank Lori Kohlstaedt and James Pesavento for mass spectrometry analysis, James Pesavento for suggesting the heavy isotopic form of ATP for mapping modified residues, Tatjana Petojevic for help with baculovirus infections, and all the members of the M.R.B. laboratory for their support and discussions. National Institutes of Health Grant CA R37-30490 (to M.R.B.) and in part Estonian Science Foundation Grant ETF9155 (to I.I.) provided financial support.

1. Méchali M (2010) Eukaryotic DNA replication origins: Many choices for appropriate answers. *Nat Rev Mol Cell Biol* 11:728–738.
2. Ilves I, Petojevic T, Pesavento JJ, Botchan MR (2010) Activation of the MCM2-7 helicase by association with Cdc45 and GINS proteins. *Mol Cell* 37:247–258.
3. Kang YH, Galal WC, Farina A, Tappin I, Hurwitz J (2012) Properties of the human Cdc45/Mcm2-7/GINS helicase complex and its action with DNA polymerase epsilon in rolling circle DNA synthesis. *Proc Natl Acad Sci USA* 109:6042–6047.
4. Moyer SE, Lewis PW, Botchan MR (2006) Isolation of the Cdc45/Mcm2-7/GINS (CMG) complex, a candidate for the eukaryotic DNA replication fork helicase. *Proc Natl Acad Sci USA* 103:10236–10241.
5. Evrin C, et al. (2009) A double-hexameric MCM2-7 complex is loaded onto origin DNA during licensing of eukaryotic DNA replication. *Proc Natl Acad Sci USA* 106: 20240–20245.
6. Remus D, et al. (2009) Concerted loading of Mcm2-7 double hexamers around DNA during DNA replication origin licensing. *Cell* 139:719–730.
7. Yardimci H, Loveland AB, Habuchi S, van Oijen AM, Walter JC (2010) Uncoupling of sister replisomes during eukaryotic DNA replication. *Mol Cell* 40:834–840.
8. Botchan M, Berger J (2010) DNA replication: Making two forks from one pre-replication complex. *Mol Cell* 40:860–861.
9. Costa A, et al. (2011) The structural basis for MCM2-7 helicase activation by GINS and Cdc45. *Nat Struct Mol Biol* 18:471–477.
10. Gambus A, et al. (2006) GINS maintains association of Cdc45 with MCM in replisome progression complexes at eukaryotic DNA replication forks. *Nat Cell Biol* 8:358–366.
11. Pacek M, Tutter AV, Kubota Y, Takisawa H, Walter JC (2006) Localization of MCM2-7, Cdc45, and GINS to the site of DNA unwinding during eukaryotic DNA replication. *Mol Cell* 21:581–587.
12. Labib K (2010) How do Cdc7 and cyclin-dependent kinases trigger the initiation of chromosome replication in eukaryotic cells? *Genes Dev* 24:1208–1219.
13. Lopez-Mosqueda J, et al. (2010) Damage-induced phosphorylation of Sld3 is important to block late origin firing. *Nature* 467:479–483.
14. Zegerman P, Diffley JF (2010) Checkpoint-dependent inhibition of DNA replication initiation by Sld3 and Dbf4 phosphorylation. *Nature* 467:474–478.
15. Berens TJ, Toczyski DP (2012) Keeping it together in times of stress: Checkpoint function at stalled replication forks. *Mol Cell* 45:585–586.
16. De Piccoli G, et al. (2012) Replisome stability at defective DNA replication forks is independent of S phase checkpoint kinases. *Mol Cell* 45:696–704.
17. Painter RB, Young BR (1975) X-ray-induced inhibition of DNA synthesis in Chinese hamster ovary, human HeLa, and Mouse L cells. *Radiat Res* 64:648–656.
18. Painter RB, Young BR (1980) Radiosensitivity in ataxia-telangiectasia: A new explanation. *Proc Natl Acad Sci USA* 77:7315–7317.
19. Watanabe I (1974) Radiation effects on DNA chain growth in mammalian cells. *Radiat Res* 58:541–556.
20. Bartkova J, et al. (2005) DNA damage response as a candidate anti-cancer barrier in early human tumorigenesis. *Nature* 434:864–870.
21. Gorgoulis VG, et al. (2005) Activation of the DNA damage checkpoint and genomic instability in human precancerous lesions. *Nature* 434:907–913.
22. Ciccia A, Elledge SJ (2010) The DNA damage response: Making it safe to play with knives. *Mol Cell* 40:179–204.
23. Sancar A, Lindsey-Boltz LA, Unsal-Kaçmaz K, Linn S (2004) Molecular mechanisms of mammalian DNA repair and the DNA damage checkpoints. *Annu Rev Biochem* 73: 39–85.
24. Stracker TH, Usui T, Petrini JH (2009) Taking the time to make important decisions: The checkpoint effector kinases Chk1 and Chk2 and the DNA damage response. *DNA Repair (Amst)* 8:1047–1054.
25. Boos D, et al. (2011) Regulation of DNA replication through Sld3-Dpb11 interaction is conserved from yeast to humans. *Curr Biol* 21:1152–1157.
26. Costanzo V, et al. (2003) An ATR- and Cdc7-dependent DNA damage checkpoint that inhibits initiation of DNA replication. *Mol Cell* 11:203–213.
27. Heffernan TP, et al. (2007) Cdc7-Dbf4 and the human S checkpoint response to UVC. *J Biol Chem* 282:9458–9468.
28. Lin DI, Aggarwal P, Diehl JA (2008) Phosphorylation of MCM3 on Ser-112 regulates its incorporation into the MCM2-7 complex. *Proc Natl Acad Sci USA* 105:8079–8084.
29. Sheu YJ, Stillman B (2010) The Dbf4-Cdc7 kinase promotes S phase by alleviating an inhibitory activity in Mcm4. *Nature* 463:113–117.
30. Li J, et al. (2011) Phosphorylation of MCM3 protein by cyclin E/cyclin-dependent kinase 2 (Cdk2) regulates its function in cell cycle. *J Biol Chem* 286:39776–39785.
31. Cortez D, Glick G, Elledge SJ (2004) Minichromosome maintenance proteins are direct targets of the ATM and ATR checkpoint kinases. *Proc Natl Acad Sci USA* 101: 10078–10083.
32. Yoo HY, Shevchenko A, Shevchenko A, Dunphy WG (2004) Mcm2 is a direct substrate of ATM and ATR during DNA damage and DNA replication checkpoint responses. *J Biol Chem* 279:53353–53364.
33. Ishimi Y, Komamura-Kohno Y, Kwon HJ, Yamada K, Nakanishi M (2003) Identification of MCM4 as a target of the DNA replication block checkpoint system. *J Biol Chem* 278: 24644–24650.
34. Matsuoka S, et al. (2007) ATM and ATR substrate analysis reveals extensive protein networks responsive to DNA damage. *Science* 316:1160–1166.
35. Shi Y, et al. (2007) Identification of carboxyl-terminal MCM3 phosphorylation sites using polyreactive phosphospecific antibodies. *J Biol Chem* 282:9236–9243.
36. Huang N, et al. (2011) Baculovirus infection induces a DNA damage response that is required for efficient viral replication. *J Virol* 85:12547–12556.
37. Schultz KL, Friesen PD (2009) Baculovirus DNA replication-specific expression factors trigger apoptosis and shutoff of host protein synthesis during infection. *J Virol* 83: 11123–11132.
38. Holt LJ, et al. (2009) Global analysis of Cdk1 substrate phosphorylation sites provides insights into evolution. *Science* 325:1682–1686.
39. Chang YP, Wang G, Bermudez V, Hurwitz J, Chen XS (2007) Crystal structure of the GINS complex and functional insights into its role in DNA replication. *Proc Natl Acad Sci USA* 104:12685–12690.
40. Choi JM, Lim HS, Kim JJ, Song OK, Cho Y (2007) Crystal structure of the human GINS complex. *Genes Dev* 21:1316–1321.
41. Kamada K, Kubota Y, Arata T, Shindo Y, Hanaoka F (2007) Structure of the human GINS complex and its assembly and functional interface in replication initiation. *Nat Struct Mol Biol* 14:388–396.
42. Brewster AS, Chen XS (2010) Insights into the MCM functional mechanism: Lessons learned from the archaeal MCM complex. *Crit Rev Biochem Mol Biol* 45:243–256.
43. Costa A, Onesti S (2009) Structural biology of MCM helicases. *Crit Rev Biochem Mol Biol* 44:326–342.
44. Brodsky MH, et al. (2004) Drosophila melanogaster MNK/Chk2 and p53 regulate multiple DNA repair and apoptotic pathways following DNA damage. *Mol Cell Biol* 24:1219–1231.
45. Peters M, et al. (2002) Chk2 regulates irradiation-induced, p53-mediated apoptosis in Drosophila. *Proc Natl Acad Sci USA* 99:11305–11310.
46. Wichmann A, Jaklevic B, Su TT (2006) Ionizing radiation induces caspase-dependent but Chk2- and p53-independent cell death in Drosophila melanogaster. *Proc Natl Acad Sci USA* 103:9952–9957.
47. Serber Z, Ferrell JE, Jr. (2007) Tuning bulk electrostatics to regulate protein function. *Cell* 128:441–444.
48. Lydeard JR, et al. (2010) Break-induced replication requires all essential DNA replication factors except those specific for pre-RC assembly. *Genes Dev* 24:1133–1144.
49. Hashimoto Y, Puddu F, Costanzo V (2012) RAD51- and MRE11-dependent reassembly of uncoupled CMG helicase complex at collapsed replication forks. *Nat Struct Mol Biol* 19:17–24.
50. Antoni L, Sodha N, Collins I, Garrett MD (2007) CHK2 kinase: Cancer susceptibility and cancer therapy - Two sides of the same coin? *Nat Rev Cancer* 7:925–936.
51. Kwak EL, et al. (2006) Mammary tumorigenesis following transgenic expression of a dominant negative CHK2 mutant. *Cancer Res* 66:1923–1928.
52. Bahassi EM, et al. (2009) Mice with the *CHEK2**1100delC SNP are predisposed to cancer with a strong gender bias. *Proc Natl Acad Sci USA* 106:17111–17116.